GEOCHEMICAL EXCHANGES ACROSS MAGMATIC INTERACTION BOUNDARIES WITHIN THE VINALHAVEN ISLAND PLUTON

NOAH WESTGATE
Department of Geology, Pomona College
Faculty Sponsors: Robert A. Wiebe, Franklin & Marshall College,
Eric Grosfils, Pomona College

INTRODUCTION

Geological occurrences such as pillow mound formations, composite dikes, and pipe formations are commonly found along the central and southern coastline of Vinalhaven Island. In each case, magmas of contrasting compositions came in contact upon the floor of the magma chamber (Weibe, 1993) to form boundaries across which chemical reactions often appear to have taken place. The aim of this study is to observe and describe the mineralogical occurrences and geochemical exchanges that occur at a variety of reaction boundaries between compositionally distinct magmas found within the lower regions of the Vinalhaven Island pluton.

FIELD RELATIONS

Seven coastal sampling locations were chosen across the southern and eastern quadrant of Vinalhaven Island (Figure 1). Samples taken include contacts found within a composite dike, several pillow mounds of contrasting compositions (Location # 4), granitic pipes rising into a gabbroic section (Location #5), and a gabbroic pillow which acted as a tube for infilling granitic magma (Wiebe, 1993; Wiebe, pers. comm.). Samples taken from Locations #4 and #5 will be discussed in this paper. Location #4 is approximately 100 m west of the southern tip of Arey Neck. It provides an example of chilled gabbroic pillows within a diorite matrix, and appears to have been emplaced on top of an older gabbroic layer with pillow formations at its bottom. Sample #4A is a chilled gabbroic pillow that has strong quenching along its exterior contact with the surrounding diorite. Brittle fracture through the gabbro was infilled with a felsic magma. Location #5 is on Coombs Neck, and shows many examples of granitic pipes rising into an overlying gabbroic flow. This gabbroic section grades outwards from the pipe formations into pillow formations emplaced within the coarse-grained granitic matrix. Pipe sample #5A has a granitic center with a leucocratic rim and pegmatites formed on one side. This suggests

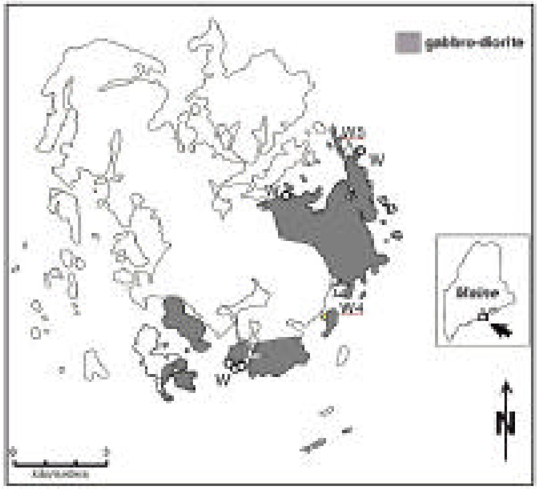

Figure 1. Map showing field sites #4 (W4) and #5 (W5). Other sampling sites marked by oW. modified after Gates, 2000

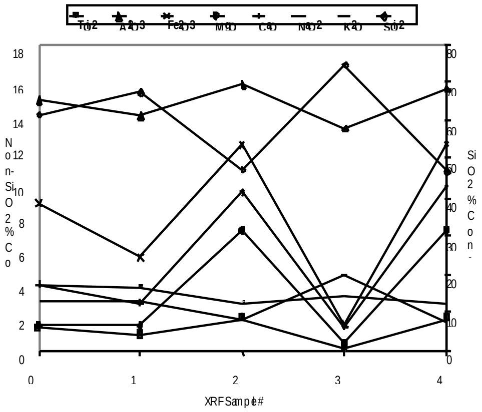

Figure 3. #4 Major Elements

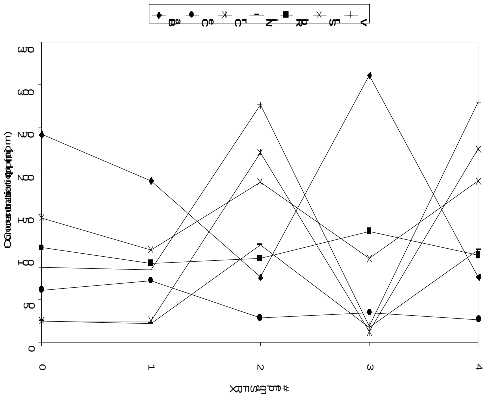

Figure 3. #4 Trace Elements

that the pipe cooled and solidified at an angle llowing for volatiles and lighter elements to rise and crystallize preferentially against its upper side.

PETROGRAPHY

This sample shows clear petrographic distinctions between the initial magmatic contact boundaries and the boundaries which formed later due to brittle fracture. The exterior edge of the gabbroic pillow shows crenulate margins and very fine grain sizes, indicative of rapid cooling as it was quenched against the lower temperature diorite. An abundance of fine-grained anhedral pyroxene, plagioclase, and quartz occur directly along the interior margins of the quenched gabbro. Fine-grained subhedral biotite is heavily concentrated within with this quenched zone, as is amphibole. Biotite abundance begins to decrease ~3 mm from the crenulated margin, and becomes virtually absent beyond ~9 mm from the diorite. Biotite is often absent in the in the gabbro immediate immediately at the contact (<0.5 mm from contact). Grain sizes increase into the interior of the gabbro, with tabular plagioclase up to ~1.5 mm in length. Olivine is found in trace proportions within the gabbro. Moving across the margin to the diorite side there is a thin (~0.4 mm) zone of subhedral quartz, plagioclase, and pyroxenes directly upon the contact boundary that shows smaller crystal sizes than are generally found within the rest of the gabbro. Beyond this narrow zone, a roughly 5 mm zone of quartz, plagioclase, and alkali feldspar grades into the diorite, with an increase in biotite, amphibole, pyroxenes, and opaque minerals further from the contact. No alkali feldspar is found at the immediate boundaries of either the initial gabbroic contact or the subsequent brittle fracture, although it can be found <0.5 mm from both. Granophyric texture is found within the diorite within crystals that border quartz, alkali feldspar, and plagioclase. The later forming brittle fracture of the gabbro pillow created a sharper contact boundary against a felsic seam composed predominantly of quartz and alkali feldspar. This fractured gabbro has no change in grain size from the contact inwards, and tabular plagioclase is found up to the fracture boundary. Biotite is concentrated along a zone from the fractured contact boundary to ~1 cm into the gabbro.

Large, poikilitic crystals of quartz, alkali feldspar, and (smaller) plagioclase are found throughout the center of this pipe. Euhedral to subhedral clinopyroxenes and minor biotite are commonly found within these large oikocrysts. Felsic grain size increases into the pegmatites found against the upper side of the pipe. Both the upper and the lower contact boundaries grade unevenly into the hybridized surroundings in which clinopyroxenes are the primary mafic mineral. There appears to be a greater abundance of pyroxene at the lower contact, although the pyroxenes at the upper contact appear somewhat larger and of more euhedral form. The largest clinopyroxene crystals are found sparsely within the pipe interior and show better form than those seen in the gabbro. A zone of biotite, and opaque minerals is found within the gabbro approximately 0.6 cm from the lower contact boundary, and is otherwise completely absent in the gabbro nearer the contact boundary.

GEOCHEMISTRY

Previous studies have shown that major transfer of K, Rb, Ca, Sr, and Na can occur across the boundaries of coexisting magmas found within a composite dike (Wiebe, 1973). Following a similar approach as Wiebe (1973), the compositional proportions of the ten major elements and nineteen trace elements were analyzed across the variety of contact boundaries within samples #4A and #5A. Table 1 shows the results of these analyses.

Table 1. XRF Major and Trace Analyses, Samples #4, #5

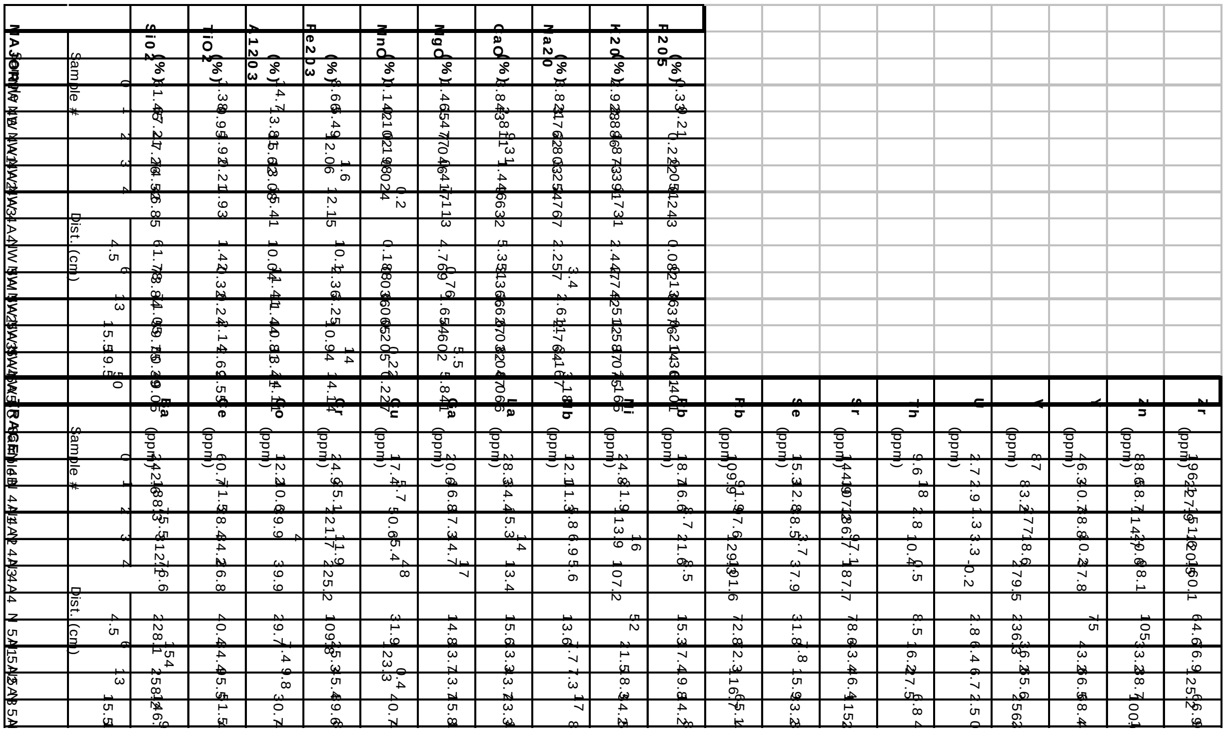

MAJORS	Sample #	SiO2 (%)	TiO2 (%)	Al2O3 (%)	Fe2O3 (%)	MnO (%)	MgO (%)	CaO (%)	Na2O (%)	K2O (%)	P2O5 (%)
[illegible]	0	[illegible]	[illegible]	[illegible]	[illegible]	[illegible]	[illegible]	[illegible]	[illegible]	[illegible]	[illegible]
[illegible]	1	[illegible]	[illegible]	[illegible]	[illegible]	[illegible]	[illegible]	[illegible]	[illegible]	[illegible]	[illegible]
[illegible]	2	[illegible]	[illegible]	[illegible]	[illegible]	[illegible]	[illegible]	[illegible]	[illegible]	[illegible]	[illegible]
[illegible]	3	[illegible]	[illegible]	[illegible]	[illegible]	[illegible]	[illegible]	[illegible]	[illegible]	[illegible]	[illegible]
[illegible]	4	[illegible]	[illegible]	[illegible]	[illegible]	[illegible]	[illegible]	[illegible]	[illegible]	[illegible]	[illegible]
	Dist. (cm)										
[illegible]	4.5	[illegible]	[illegible]	[illegible]	[illegible]	[illegible]	[illegible]	[illegible]	[illegible]	[illegible]	[illegible]
[illegible]	6	[illegible]	[illegible]	[illegible]	[illegible]	[illegible]	[illegible]	[illegible]	[illegible]	[illegible]	[illegible]
[illegible]	13	[illegible]	[illegible]	[illegible]	[illegible]	[illegible]	[illegible]	[illegible]	[illegible]	[illegible]	[illegible]
[illegible]	15.5	[illegible]	[illegible]	[illegible]	[illegible]	[illegible]	[illegible]	[illegible]	[illegible]	[illegible]	[illegible]
[illegible]	[illegible]	[illegible]	[illegible]	[illegible]	[illegible]	[illegible]	[illegible]	[illegible]	[illegible]	[illegible]	[illegible]

TRACE	Sample #	Ba (ppm)	Ce (ppm)	Co (ppm)	Cr (ppm)	Cu (ppm)	Ga (ppm)	La (ppm)	Nb (ppm)	Ni (ppm)	Pb (ppm)	Rb (ppm)	Sc (ppm)	Sr (ppm)	Th (ppm)	U (ppm)	V (ppm)	Y (ppm)	Zn (ppm)	Zr (ppm)
[illegible]	0	[illegible]	[illegible]	[illegible]	[illegible]	[illegible]	[illegible]	[illegible]	[illegible]	[illegible]	[illegible]	[illegible]	[illegible]	[illegible]	[illegible]	[illegible]	[illegible]	[illegible]	[illegible]	[illegible]
[illegible]	1	[illegible]	[illegible]	[illegible]	[illegible]	[illegible]	[illegible]	[illegible]	[illegible]	[illegible]	[illegible]	[illegible]	[illegible]	[illegible]	[illegible]	[illegible]	[illegible]	[illegible]	[illegible]	[illegible]
[illegible]	2	[illegible]	[illegible]	[illegible]	[illegible]	[illegible]	[illegible]	[illegible]	[illegible]	[illegible]	[illegible]	[illegible]	[illegible]	[illegible]	[illegible]	[illegible]	[illegible]	[illegible]	[illegible]	[illegible]
[illegible]	3	[illegible]	[illegible]	[illegible]	[illegible]	[illegible]	[illegible]	[illegible]	[illegible]	[illegible]	[illegible]	[illegible]	[illegible]	[illegible]	[illegible]	[illegible]	[illegible]	[illegible]	[illegible]	[illegible]
[illegible]	4	[illegible]	[illegible]	[illegible]	[illegible]	[illegible]	[illegible]	[illegible]	[illegible]	[illegible]	[illegible]	[illegible]	[illegible]	[illegible]	[illegible]	[illegible]	[illegible]	[illegible]	[illegible]	[illegible]
	Dist. (cm)																			
[illegible]	4.5	[illegible]	[illegible]	[illegible]	[illegible]	[illegible]	[illegible]	[illegible]	[illegible]	[illegible]	[illegible]	[illegible]	[illegible]	[illegible]	[illegible]	[illegible]	[illegible]	[illegible]	[illegible]	[illegible]
[illegible]	6	[illegible]	[illegible]	[illegible]	[illegible]	[illegible]	[illegible]	[illegible]	[illegible]	[illegible]	[illegible]	[illegible]	[illegible]	[illegible]	[illegible]	[illegible]	[illegible]	[illegible]	[illegible]	[illegible]
[illegible]	13	[illegible]	[illegible]	[illegible]	[illegible]	[illegible]	[illegible]	[illegible]	[illegible]	[illegible]	[illegible]	[illegible]	[illegible]	[illegible]	[illegible]	[illegible]	[illegible]	[illegible]	[illegible]	[illegible]
[illegible]	15.5	[illegible]	[illegible]	[illegible]	[illegible]	[illegible]	[illegible]	[illegible]	[illegible]	[illegible]	[illegible]	[illegible]	[illegible]	[illegible]	[illegible]	[illegible]	[illegible]	[illegible]	[illegible]	[illegible]

Eight major element percent concentrations (Si, Ti, Al, Fe, Mg, Ca, Na, and K) and seven trace element concentrations (Ba, Ce, Cr, Ni, Rb, Sr, and V) are represented graphically in Figures 2 and 3. On these graphs, XRF sample #0 represents the diorite end-member composition (#4B). XRF sample #1 represents diorite located ~4 cm from the tip of the pillow in sample #4A. XRF sample #2 represents the the tip of the gabbroic pillow up to its contact with the surrounding dioritic groundmass. XRF sample #3 represents felsic seam found within the brittle fracture of the gabbroic pillow. XRF sample #4 represents the interior of this gabbroic pillow where it is >1.5 cm from the contact boundary with the diorite.

The same eight major element concentrations and seven trace element concentrations are represented graphically for sample #5A in Figures 4 and 5. The XRF samples were taken in a straight line across sample #5A perpendicular to the orientation of the pipe and are graphed as a function of their relative distance from each other and the margins of sample #5A. The first XRF sample represents the hybridized gabbro found at the upper side of the pipe contact. The second XRF sample represents the pegmatitic pipe exterior found on the other side of this contact. The third XRF sample represents the lower pipe interior up to the lower contact margin. The fourth XRF sample represents the hybridized gabbro found on the other side of this contact boundary. The fifth XRF sample represents the furthest gabbro from the pipe found within this sample.

DISCUSSION

By performing XRF major and trace element analysis at points directly bordering contact boundaries as well as points further from those contact boundaries, comparisons can be made between the two and hypotheses about geochemical exchanges can be explored. Such comparisons in samples #4 and #5 show some interesting trends. In sample #5A, gabbro found near the contact boundaries with the pipe appears to have been enriched in K, Si, Rb, Ba, Cr, and Ce, and depleted in Ti, Al, Fe, Mg, Ca, Na, Sr, Ni, and V. The gabbro found at the upper contact boundary against the pegmatitic side of the pipe generally shows greater levels of geochemical enrichment and depletion than does the gabbro bordering the lower, non-pegmatitic pipe (the only exceptions being Mg, Ce, and Ni). This is strongly suggests that a greater level of geochemical exchange occurred along the upper edge of the angled pipe. The granite at these contact boundaries shows enrichment in Si, Na, and Ti, and depletion in K, Rb, Ba, Cr, Ce, Sr, V, Ca, Fe, and Mg. The fractionation of dioritic and granitic material found in samples #4 and #5 may be largely responsible for much of the geochemical variation observed (Wiebe, pers. comm.). The petrographic and geochemical evidence provided here does however indicate that significant levels of geochemical exchange took place across the boundaries formed during the initial contact of these compositionally distinct magmas. In sample #4, the presence of abundant biotite within the chilled gabbro indicates significant exchange from the diorite into the gabbro, and is supported by the lack of alkali feldspar in the diorite directly at the boundary (Wiebe, 1973). The smaller crystal sizes found within this thin zone may be explained by H2O transfer from the diorite into the gabbro which would slow diffusion and increase the rate of nucleation, thereby forming smaller crystal sizes (Wiebe, pers. comm.). While no rapid crystallization is observed along the fractured gabbro boundary, the higher proportion of biotite on the gabbro side of the contact indicates that some amount of geochemical exchange occured across this brittle fracture margin. This indicates that while higher levels of geochemical exchanges occurred early on during liquid-liquid contact, exchange continued after the gabbro had solidified to a point in which brittle fracture was possible. (Wiebe, 1973). Geochemical exchanges appear to have had a significant effect on the compositional diversity found across mafic and felsic contact boundaries (Mitchell & Rhodes, 1989).

Figure 5. #5 Major Elements

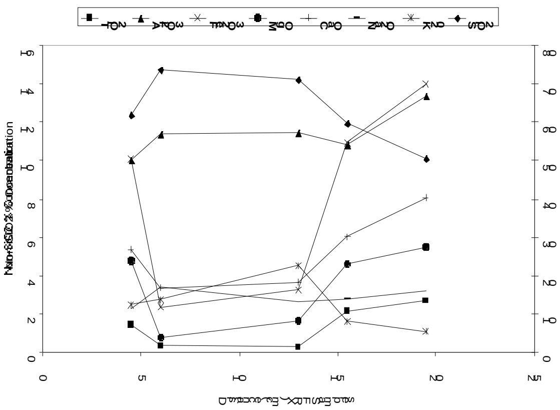

Figure 5. #5 Trace Elements

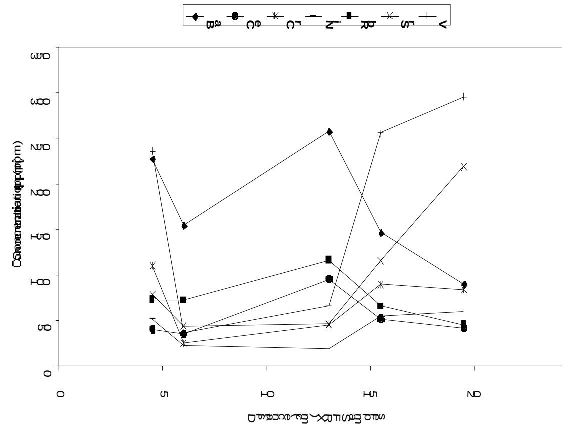

REFERENCE

Wiebe R. A., 1973, Relations Between Coexisting Basaltic and Granitic Magmas in a Composite Dike" American Journal of Science, Vol. 273, February, p. 130-151

Wiebe R.A., 1993, Basaltic Injections into Floored Silicic Magma Chambers, Eos, Tran., AGU, Vol 74, No.1, January 05, p. 01 and 03

Mitchell C. B., & Rhodes J. M., 1989, Geochemistry of the Granite-Gabbro Complex on Vinalhaven Island, Maine, Maine Geological Survey; Studies in Maine Geology, Volume 4,. p. 45-57

Gates, O., 2000, Geologic map of Vinalhaven Island. Maine Geological Survey, Department of Conservation